ORIGINAL LABORATORY RESEARCH REPORT

OPEN

Reactive Oxygen Species Contributes to Type 2 Diabetic Neuropathic Pain via the Thioredoxin-Interacting Protein-NOD–Like Receptor Protein 3-*N*-Methyl-D-Aspartic Acid Receptor 2B Pathway

Jun-Wu Wang, BD,* Xiu-Ying Ye, BD,* Ning Wei, BD,* Shi-Shu Wu, BD,* Zhe-Hao Zhang, BD,* Guang-Hui Luo, BD,* Xu Li, PhD,† Jun Li, PhD, MD,* and Hong Cao, MD*

BACKGROUND: The number of patients with diabetic neuropathic pain (DNP) continues to increase, but available treatments are limited. This study aimed to examine the influence of reactive oxygen species (ROS)-thioredoxin-interacting protein (TXNIP)-NOD–like receptor protein 3 (NLRP3)-*N*-methyl-D-aspartic acid receptor 2B (NR2B) pathway on type 2 DNP.

METHODS: Male Sprague-Dawley rats were fed with a high-fat and high-sugar diet for 8 weeks. Then, rats were intraperitoneally injected with streptozotocin (STZ, 35 mg/kg) to induce type 2 diabetes mellitus in rats. Diabetic rats with <85% of their basic levels in mechanical withdrawal threshold and thermal withdrawal latency were classified as DNP rats on day 14 after STZ injection. DNP rats were treated with ROS scavenger N-tert-Butyl-α-phenylnitrone (PBN, 100 $mg \cdot kg^{-1} \cdot d^{-1}$) or TXNIP small interfering ribonucleic acid (10 μg/d) once daily for 14 days. The level of ROS, protein levels of NLRP3, TXNIP, cysteinyl aspartate-specific proteinase-1 (caspase-1), interleukin-1β (IL-1β), NR2B phosphorylation at Tyr1472 (p-NR2B), total NR2B (t-NR2B), and distribution of NLRP3 in the spinal cord were examined. In vitro experiments, BV2 cells and PC12 cells were individually cultured and cocultured in a high-glucose environment (35 mmol/L D-glucose). The level of ROS and protein levels of NLRP3, TXNIP, caspase-1, and IL-1β in BV2 cells, and p-NR2B, t-NR2B in PC12 cells were detected. The level of ROS was detected by the flow cytometry approach. The protein levels were detected by the Western blot technique. The location of NLRP3 was observed by immunofluorescent staining. The interaction between TXNIP and NLRP3 was detected by coimmunoprecipitation assay.

RESULTS: The level of spinal ROS increased in DNP rats. The mechanical allodynia and thermal hyperalgesia of DNP rats were alleviated after systemic administration of PBN. This administration decreased protein levels of NLRP3, TXNIP, caspase-1, IL-1β, and p-NR2B and the coupling of TXNIP to NLRP3 in spinal cords of DNP rats. Furthermore, knockdown of spinal TXNIP alleviated nociceptive hypersensitivity and decreased protein levels of NLRP3, TXNIP, caspase-1, IL-1β, and p-NR2B in DNP rats. The level of ROS and protein levels of NLRP3, TXNIP, caspase-1, IL-1β, the coupling of TXNIP to NLRP3, and the IL-1β secretion increased in BV2 cells, and the protein expression of p-NR2B increased in cocultured PC12 cells in a high-glucose environment. All of these in vitro effects were significantly blocked after treatment of PBN.

CONCLUSIONS: Our findings suggest that spinal ROS can contribute to type 2 DNP through TXNIP-NLRP3-NR2B pathway. (Anesth Analg 2022;135:865–76)

KEY POINTS

- **Question:** Does reactive oxygen species (ROS) contribute to diabetic neuropathic pain (DNP) via the activation of the thioredoxin-interacting protein (TXNIP)-NOD–like receptor protein 3 (NLRP3)-N-methyl-D-aspartic acid receptor 2B (NR2B) pathway in type 2 DNP rats?
- **Findings:** This study demonstrated that the activation of the ROS-TXNIP-NLRP3 pathway in microglia promoted interleukin-1β (IL-1β) release and increased NR2B phosphorylation in neurons, leading to mechanical allodynia and thermal hyperalgesia in type 2 DNP rats.
- **Meaning:** Targeting individual inflammasome components and their activators such as ROS and TXNIP may be an alternative approach for treating type 2 DNP.

From the *Department of Anesthesiology, The Second Affiliated Hospital and Yuying Children's Hospital, Pain Medicine Institute, Wenzhou Medical University, Zhejiang, China; and †Basic Medicine College of Wenzhou Medical University, Zhejiang, China.

Accepted for publication May 6, 2022.

DOI: 10.1213/ANE.0000000000006117

Funding: This study was supported by the National Natural Science Foundation of China (project no. 81771487).

The authors declare no conflicts of interest.

J.-W. Wang and X.-Y. Ye contributed equally and share first authorship.

Supplemental digital content is available for this article. Direct URL citations appear in the printed text and are provided in the HTML and PDF versions of this article on the journal's website (www.anesthesia-analgesia.org).

Reprints will not be available from the authors.

Address correspondence to Hong Cao, MD, Department of Anesthesiology, The Second Affiliated Hospital and Yuying Children's Hospital, Pain Medicine Institute, Wenzhou Medical University, No. 109, West College Rd, Lucheng, Zhejiang 325027, China. Address e-mail to caohongwz@163.com.

GLOSSARY

ANOVA = analysis of variance; **BV2** = mouse microglia cell line BV2; **C group** = control group; **caspase-1** = cysteinyl aspartate-specific proteinase-1; **CCI** = chronic constriction injury; **DCFH-DA** = 2',7'-dichlorodihydrofluoroscein diacetate; **DM** = diabetes mellitus; **DMSO** = dimethyl sulfoxide; **DNP** = diabetic neuropathic pain; **ELISA** = enzyme-linked immunosorbent assay; **FITC** = fluorescein isothiocyanate; **GFAP** = glial fibrillary acidic protein; **HFSD** = high-fat and high-sugar diet; **Iba** = ionized calcium-binding adaptor protein; **IENF** = intraepidermal nerve fibers; **IL-1β** = interleukin-1β; **mtROS** = mitochondrial reactive oxygen species; **MWT** = mechanical withdrawal threshold; **NC** = negative control; **ND** = normal diet; **NeuN** = neuronal nuclei; **NLRP3** = NOD-like receptor protein 3; **NMDAR** = *N*-methyl-D-aspartate receptor; **NR2B** = *N*-methyl-D-aspartic acid receptor 2B; **PBN** = N-tert-Butyl-α-phenylnitrone; **PBS** = phosphate-buffered saline; **PC12** = rat neuron cell line PC12; **PL group** = painless group; **PMSF** = phenylmethanesulfonyl fluoride; **p-NR2B** = NR2B phosphorylation at Tyr1472; **PVDF** = polyvinylidene fluoride; **RIPA** = radio immunoprecipitation assay; **ROS** = reactive oxygen species; **SC** = solvent control; **SDS-PAGE** = sodium dodecyl sulfate polyacrylamide gel electrophoresis; **siRNA** = small interfering ribonucleic acid; **STZ** = streptozotocin; **t-NR2B** = total NR2B; **TRX** = thioredoxin; **TWL** = thermal withdrawal latency; **TXNIP** = thioredoxin-interacting protein

It was estimated that about 463 million people suffered from diabetes in 2019,[1] 90% of whom had type 2 diabetes mellitus (DM).[2] About a third of diabetic patients develop diabetic neuropathic pain (DNP).[3]

Neuropathic pain genesis is related to glutamatergic signal activation, glial activation, proinflammatory cytokines production, and disinhibition in the spinal cord.[4] Activated microglia releases various neuromodulators and neuroactive substances, such as reactive oxygen species (ROS), which activate spinal *N*-methyl-D-aspartate receptor (NMDAR).[5] There is compelling evidence for the involvement of spinal NMDAR in the development of neuropathic pain.[6,7] Our previous study identified that the *N*-methyl-D-aspartic acid receptor 2B (NR2B) subunits of NMDAR played a vital role in the development of DNP. Blocking spinal NMDAR attenuated DNP.[8] Spinal NMDAR is likely a primary target for the treatment of neuropathic pain.[9] However, the side effects of NMDAR antagonists limit their application. Thus, safer and more effective therapies based on mechanistic targets to DNP are urgently required.

One of the primary questions that must be addressed is what mechanisms trigger NR2B activation in the DNP. Several recent studies revealed that ROS was associated with NMDAR activation.[10,11] Our previous study demonstrated that ROS played a vital role in generating DNP.[12] However, the mechanisms by which ROS is linked to spinal NR2B phosphorylation at Tyr1472 (p-NR2B) under DNP conditions are still unknown.

Activation of NOD-like receptor protein 3 (NLRP3) inflammasome promotes the maturation and secretion of interleukin-1β (IL-1β) by activating the cysteinyl aspartate-specific proteinase-1 (caspase-1). It has been well documented that NLRP3 participates in neuropathic pain.[13–15] Furthermore, the administration of NLRP3 inflammasome inhibitor attenuated nerve injury-induced mechanical allodynia.[16] ROS has also been shown to play a vital role in activating the NLRP3 inflammasome.[17,18]

However, it remains unknown whether ROS contributes to neuropathic pain in type 2 diabetes by activating the NLRP3 inflammasome. Moreover, whether NLRP3 inflammasome is activated in the development of DNP is remained poorly defined. Thioredoxin-interacting protein (TXNIP), a redox-dependent inhibition of thioredoxin (TRX), dissociates with TRX in the presence of high concentrations of ROS.[19] Recent studies showed that TXNIP could activate the NLRP3 inflammasome in a variety of diseases including neuropathic pain.[20,21] Given that the level of TXNIP protein was regulated by ROS,[22] we proposed that ROS activated NMDAR through the TXNIP-NLRP3 pathway in the spinal cord required for the development of type 2 DNP.

METHODS

Establishment of Type 2 DM and the Animal Groups

All animal procedures were approved by the Animal Experimental Ethical Inspection of Laboratory Animal Centre, Wenzhou Medical University. The male Sprague-Dawley rats (130–150 g) were randomly divided into two groups: control group (n = 12) and DM group (n = 80). Rats in control group were fed with a normal diet (ND), and rats in DM group were fed with the high-fat and high-sugar diet (HFSD) for 8 weeks. The mechanical withdrawal threshold (MWT) and thermal withdrawal latency (TWL) of rats were measured at 8 weeks as a base level. Rats in DM group were intraperitoneally injected with streptozotocin (STZ, 35 mg/kg). Rats with fasting blood glucose levels (>16.7 mmol/L) were classified as diabetic rats on day 3 after STZ injection. Diabetic rats with <85% of basic levels in the MWT and TWL were classified as DNP rats on day 14 after STZ injection. DNP rats were randomly divided into 5 groups: DNP group (n = 12), DNP + TXNIP siRNA group (n = 12), DNP + PBN group (n = 12), solvent control group (n = 12), and negative control of siRNA group (n = 12). Diabetic rats without the development of DNP were classified as painless group

(n = 12). Since approximately 80% of type 2 diabetic rats developed type 2 DNP,[8] more rats were prepared to meet the requirements for the minimum number of animals per group. Rats in DNP + PBN group were intraperitoneally injected with ROS scavenger N-tert-Butyl-α-phenylnitrone (PBN, 100 mg·kg^{-1}·d^{-1}, Sigma-Aldrich) dissolved in 0.1% dimethyl sulfoxide (DMSO). Rats in solvent control group were intraperitoneally injected with 0.1% DMSO (2 mL·kg^{-1}·d^{-1}). Rats in DNP + TXNIP siRNA group were intrathecal injected with 10 μg/d TXNIP small interfering ribonucleic acid (siRNA, GenePharma, 5-GCUGG AUAGACCUAAACAUTT-3 [sense]; 5-AUGUUUAGGUCUAUCCAGCTT-3 [antisense]) dissolved in 10 μL Lipofectamine 2000 (Invitrogen). Rats in negative control of siRNA group were intrathecally injected with 10 μg/d negative control of siRNA (5-UUCUCCGAACGUGUCACGUTT-3 [sense]; 5-ACGUGACACGUUCGGA GAATT-3 [antisense]) dissolved in 10 μL Lipofectamine 2000 (Supplemental Digital Content, Figure 1A, http://links.lww.com/AA/E2).

Pain Behaviors

The MWT. The hind paw of rats was stimulated by the IITC 2390 electronic von Frey tactile pain measurement instrument. The maximal force was recorded when rats lifted their hind legs during the stimulation. The stimulation was repeated 3 times as their MWT.

The TWL. The TWL was measured by a plantar/tail-flick tester (IITC 336). The hind paw of rats was exposed to thermal radiation, and the time was recorded from the beginning of stimulation to the lifting of the hind paw of rats. The stimulation was repeated 3 times as their TWL.

ROS Measurement

The generation of ROS was measured by using the 2′,7′-dichlorodihydrofluoroscein diacetate (DCFH-DA) assay (Nanjing Jiancheng Bioengineering Institute). The single-cell suspension from spinal cord segments (L4-L6) was collected. The cell suspension was centrifuged at 500 g for 10 minutes. DCFH-DA (10 μM) was added to the cell suspension and incubated at 37 °C for 1 hour. The fluorescence was examined by flow cytometry (Beckman, Germany). In vitro experiments, BV2 cells were cultured in 12-well plates. BV2 cells were incubated with DCFH-DA (10 μM) at 37 °C for 20 minutes after being treated with high glucose and PBN for 24 hours. The fluorescence of fluorescein isothiocyanate (FITC) was measured using flow cytometry. The mean fluorescence intensity was analyzed using the CytExpert analysis software.

Western Blot Analysis

The spinal cord segments (L4-L6) or cells were placed in a buffer solution containing radio immunoprecipitation assay (RIPA), phenylmethanesulfonyl fluoride (PMSF), and protein phosphorylase inhibitor. The supernatant was collected after centrifugation. The proteins were separated with 12% sodium dodecyl sulfate polyacrylamide gel electrophoresis (SDS-PAGE) gels and transferred to polyvinylidene fluoride (PVDF) membranes. After being blocked with 5% nonfat milk, the membranes were incubated with the primary antibodies against p-NR2B (1:800; AB5403, Merck Millipore), total NR2B (t-NR2B, 1:1000; 4212, Cell Signaling Technology), NLRP3(1:1000; 19771-1-AP, Proteintech), TXNIP (1:1000; 14715, Cell Signaling Technology), caspase-1 (1:1000; 4199, Cell Signaling Technology), β-actin (1:1000; TA-09, Beijing Zhongshan Jinqiao Biotechnology), or IL-1β (0.2 μg/mL; ab9722, Abcam). The membranes were then incubated with the secondary antibody. The protein was detected by enhanced chemiluminescent. The target protein bands were analyzed by Quantity One software.

Immunofluorescence

Immunofluorescence labeling was performed according to our previously published method.[12] The spinal cord sections (L4-L6, 6 μm) were incubated with a mixture of NLRP3 antibody (1:50; A5652, ABclonal) and glial fibrillary acidic protein (GFAP) antibody (1:50; sc-33673, Santa Cruz), neuronal nuclei (NeuN) antibody (1:100; MAB377, Millipore), ionized calcium-binding adaptor protein (Iba) antibody (1:500; 011-27991, Wako) or a mixture of NLRP3 antibody (1:50; M035175, Abmart) and TXNIP antibody (1:50;T572136, Abmart). The spinal cord sections were incubated at 37 °C in a corresponding fluorescent secondary antibody. The fluorescent sections of the spinal cord were examined under a fluorescence microscope.

Coimmunoprecipitation

NLRP3 antibody was added to 400 μg of the lysate of the spinal cord or cells with rotation for 1 hour at 4 °C. Then, 20 μg protein A/G PLUS agarose beads were added to the tissue lysate with rotation overnight at 4 °C. After the mixture was centrifuged at 2500 rpm for 10 minutes, the precipitate was washed 3 times with phosphate-buffered saline (PBS). The precipitate was resuspended in 80 μL of Protein Loading Buffer (1X) and boiled for 10 minutes before the supernatant was collected. The protein levels of TXNIP and NLRP3 were examined by western blot assay.

Enzyme-Linked Immunosorbent Assay

The fasting serum of rats was collected, and the insulin concentration (mIU/L) was measured by enzyme-linked immunosorbent assay (ELISA) kits (Haixi Tang Biotechnology). The insulin sensitivity index was calculated by the formula: ln (1/[fasting glucose

× fasting insulin]). In vitro experiments, the supernatant was collected, and the level of IL-1β secretion was examined using ELISA assay.

Cell Cultures and Treatments

Mouse microglia cell line BV2 was obtained from Kunming cell bank, and rat neuron cell line PC12 was purchased from Shanghai BoYun Biotechnology Co, Ltd. BV2 cells and PC12 cells were maintained in Dulbecco's modified eagle's medium with 10% fetal bovine serum and 1% penicillin-streptomycin. Cells were cultured at 37 °C in a humid atmosphere with 5% CO_2. D-glucose was added into a medium for high-glucose treatment.

BV2 Cells Culture and Treatment

BV2 cells were plated at a density of 3 × 10^5 cells/well in a 6-well plate in a low-glucose medium (5.5 mmol/L D-glucose) to the logarithmic growth phase. BV2 cells were randomly divided into 5 groups: normal control group (5.5 mmol/L D-glucose), high-glucose group (35 mmol/L D-glucose), osmotic pressure control group (5.5 mmol/L D-glucose + 29.5 mmol/L mannitol), PBN group (35 mmol/L D-glucose and 200 μM PBN), and solvent control group (35 mmol/L D-glucose and 0.2% DMSO). After 24 hours of cultivation, the protein levels of NLRP3, TXNIP, caspase-1, and IL-1β in BV2 cells were examined by western blot technique. The content of IL-1β in the supernatant was measured using ELISA assay. The level of ROS in BV2 cells was examined by flow cytometry.

PC12 Cells Culture and Treatment

PC12 cells were seeded at 6 × 10^5 cells/well in a 6-well plate in a low-glucose medium (5.5 mmol/L D-glucose) to the logarithmic growth phase. PC12 cells were randomly divided into 3 groups: normal control group (5.5 mmol/L D-glucose), high-glucose group (35 mmol/L D-glucose), and osmotic pressure control group (5.5 mmol/L D-glucose + 29.5 mmol/L mannitol). 24 hours after treatments, cells were collected for examining the protein expression of p-NR2B, t-NR2B in PC12 cells by using western blot assay.

Cell Coculture Systems

The coculture of BV2 cells and PC12 cells was established by using Transwell cell cultivation of chambers. BV2 cells were plated in the upper chamber at a density of 3 × 10^5 cells/chamber with 0.8 mL medium. PC12 cells were plated in the lower chamber at a density of 6 × 10^5 cells/chamber with a 1.5 mL medium. After 24 hours, the PC12 cells were randomly divided into 4 groups: normal control cocultured group (5.5 mmol/L D-glucose), high glucose cocultured group (35 mmol/L D-glucose), PBN cocultured group (35 mmol/L D-glucose and 200 μM PBN), and solvent control cocultured group (35 mmol/L D-glucose and 0.2% DMSO). The upper chamber was added into the lower chamber. 24 hours after the coculture, the protein levels of p-NR2B, t-NR2B in PC12 cells were examined by western blot technique (Supplemental Digital Content, Figure 1B–D, http://links.lww.com/AA/E2).

Statistical Analysis

The sample size was determined by referring to previous studies without a priori power analysis. We previously used 6 to 8 rats per group for behavioral testing and 3 to 6 rats per group for western blot assay.[8,23] All data are presented as mean ± standard deviation and were analyzed using GraphPad Prism 8. The results were analyzed with a 1-way analysis of variance (ANOVA), 1-way repeated measures ANOVA, or 2-way repeated measures ANOVA. When the ANOVA exhibited a significant difference, pairwise comparisons between means were tested by using the post hoc Tukey's method or Sidak method. $P < .05$ was considered as a significant difference.

RESULTS

Induction of Type 2 Diabetic Model

Neuropathic pain is a well-recognized complication of type 2 diabetes. To determine the mechanisms of DNP, we used the HFSD/STZ-induced type 2 diabetic rat model. After 8 weeks of an HFSD, higher insulin levels and lower insulin sensitivity index of rats in DM group were examined, indicating that insulin resistance was elicited. The weight of rats in DM group increased compared with control group, while the blood glucose did not differ. On day 3 after STZ injection, the blood glucose of DM rats significantly increased and met the diagnosis criteria of type 2 diabetes (>16.7 mmol/L), suggesting the type 2 diabetic rat model was established. The weight of DM rats significantly decreased on day 14 after STZ injection (Figure 1A).

Systemic Administration of PBN Attenuated Nociceptive Hypersensitivity and Decreased Level of Spinal ROS in DNP Rats

On day 14 after STZ injection, the MWT and TWL of DNP rats in DNP group and solvent control group were lower than 85% of the basic levels ($P < .0001$). The level of ROS increased in DNP rats when compared with rats in control group and painless group on days 17, 21, and 28 after STZ injection. Systemic administration of PBN decreased ROS production in DNP rats (Figure 1B). The MWT and TWL of rats in DNP + PBN group and DNP + TXNIP siRNA group increased on days 17, 21, and 28 after STZ injection, indicating that treatment of PBN or TXNIP siRNA alleviated the mechanical allodynia and thermal hyperalgesia in DNP rats (Figure 1C). There were no significant

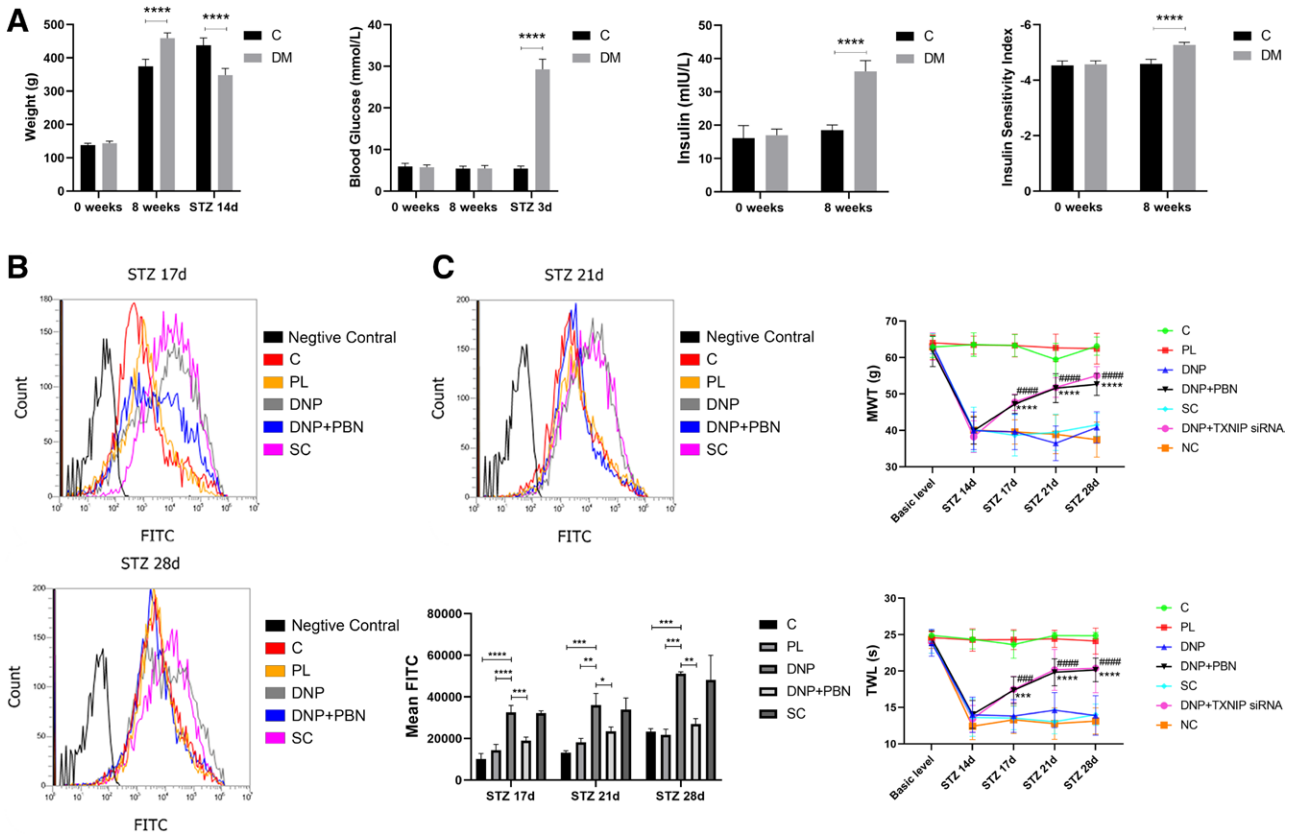

Figure 1. The type 2 diabetic neuropathic pain rat models were established, and ROS scavenger PBN reversed the nociceptive hypersensitivity and decreased ROS production in diabetic neuropathic pain rats. A, The comparison of blood glucose (0 wk: $P = .9855$; 8 wk: $P = .9991$), weight (0 wk: $P = .9295$), serum insulin levels (0 wk: $P = .8395$), and insulin sensitivity index (0 wk: $P = .8857$) between rats in the control group and diabetes mellitus group (mean ± standard deviation. n = 6. $^{****}P < .0001$, Sidak post hoc test after 2-way repeated measures ANOVA). B, The flow cytometry assay revealed the level of ROS in spinal cords of rats in each group on days 17, 21, and 28 after STZ intraperitoneal injection (mean ± standard deviation. n = 3. $^{*}P < .05$, $^{**}P < .01$, $^{***}P < .001$, and $^{****}P < .0001$. DNP group versus C group: STZ 21 d, $^{***}P = .0002$; STZ 28 d, $^{***}P = .0008$. DNP group versus PL group: STZ 21 d, $^{**}P = .0012$; STZ 28 d, $^{***}P = .0005$. DNP group versus DNP + PBN group: STZ 17 d, $^{***}P = .0004$; STZ 21 d, $^{*}P = .0142$; STZ 28 d, $^{**}P = .0023$. DNP group versus SC group: STZ 17 d, $P = .9997$; STZ 21 d, $P = .9552$; STZ 28 d, $P = .9626$. Tukey post hoc test after 1-way ANOVA). C, The TWL and MWT of rats in each group were measured. PBN reversed the nociceptive hypersensitivity on days 17, 21, and 28 after STZ intraperitoneal injection. (Mean ± standard deviation. n = 6. DNP group versus DNP + PBN group: $^{***}P = .0002$, $^{****}P < .0001$; DNP group versus DNP + TXNIP siRNA group: $^{\#\#\#}P = .0001$, $^{\#\#\#\#}P < .0001$; DNP group versus SC group: STZ 17 d, $P = .9976$ (MWT), $P = .9995$ (TWL); STZ 21 d, $P = .5235$ (MWT), $P = .2895$ (TWL); STZ 28 d, $P = .9977$ (MWT), $P > .9999$ (TWL). DNP group versus NC group: STZ 17 d, $P > .9999$ (MWT), $P = .9896$ (TWL); STZ 21 d, $P = .7709$ (MWT), $P = .2198$ (TWL); STZ 28 d, $P = .3266$ (MWT), $P = .9512$ (TWL); Tukey post hoc test after 2-way repeated measures ANOVA.) ANOVA indicates analysis of variance; C group, control group; DM group, diabetes mellitus group; DNP group, diabetic neuropathic pain group; mean FITC, mean fluorescence of fluorescein isothiocyanate; MWT, mechanical withdrawal threshold; NC group, negative control of siRNA group; PBN, N-tert-Butyl-α-phenylnitrone; PL group, painless group; ROS, reactive oxygen species; SC group, solvent control group; STZ, streptozotocin; TWL, thermal withdrawal latency; TXNIP, thioredoxin-interacting protein

differences in nociceptive hypersensitivity and levels of ROS between DNP group and solvent control group (Figure 1B, C). These results indicate that ROS contributed to the development of type 2 DNP.

PBN Decreased Phosphorylation of NR2B, NLRP3 Inflammasome Activation, and Protein Levels of TXNIP and IL-1β in DNP Rats

The protein expression of spinal p-NR2B in DNP rats significantly increased when compared with rats in control group and painless group. Systemic administration of PBN significantly blocked this increase in spinal cords of DNP rats on days 17, 21, and 28 after STZ injection. Furthermore, to determine whether ROS increased the protein levels of TXNIP and NLRP3 and activated NLRP3 inflammasome in DNP rats, the spinal protein levels of NLRP3, TXNIP, caspase-1, and IL-1β in rats in each group were measured at the same time. The spinal protein levels of NLRP3, TXNIP, caspase-1, and IL-1β in DNP rats significantly increased when compared with rats in control group and painless group. Systemic administration of PBN significantly attenuated these increases in spinal cords of DNP rats. The protein expression of spinal t-NR2B in rats among all treated groups did not differ. As expected, vehicle DMSO did not affect the levels of these proteins (Figure 2). These results indicate that ROS was involved in the increase in spinal protein levels of p-NR2B, NLRP3, TXNIP, caspase-1, and IL-1β in DNP rats.

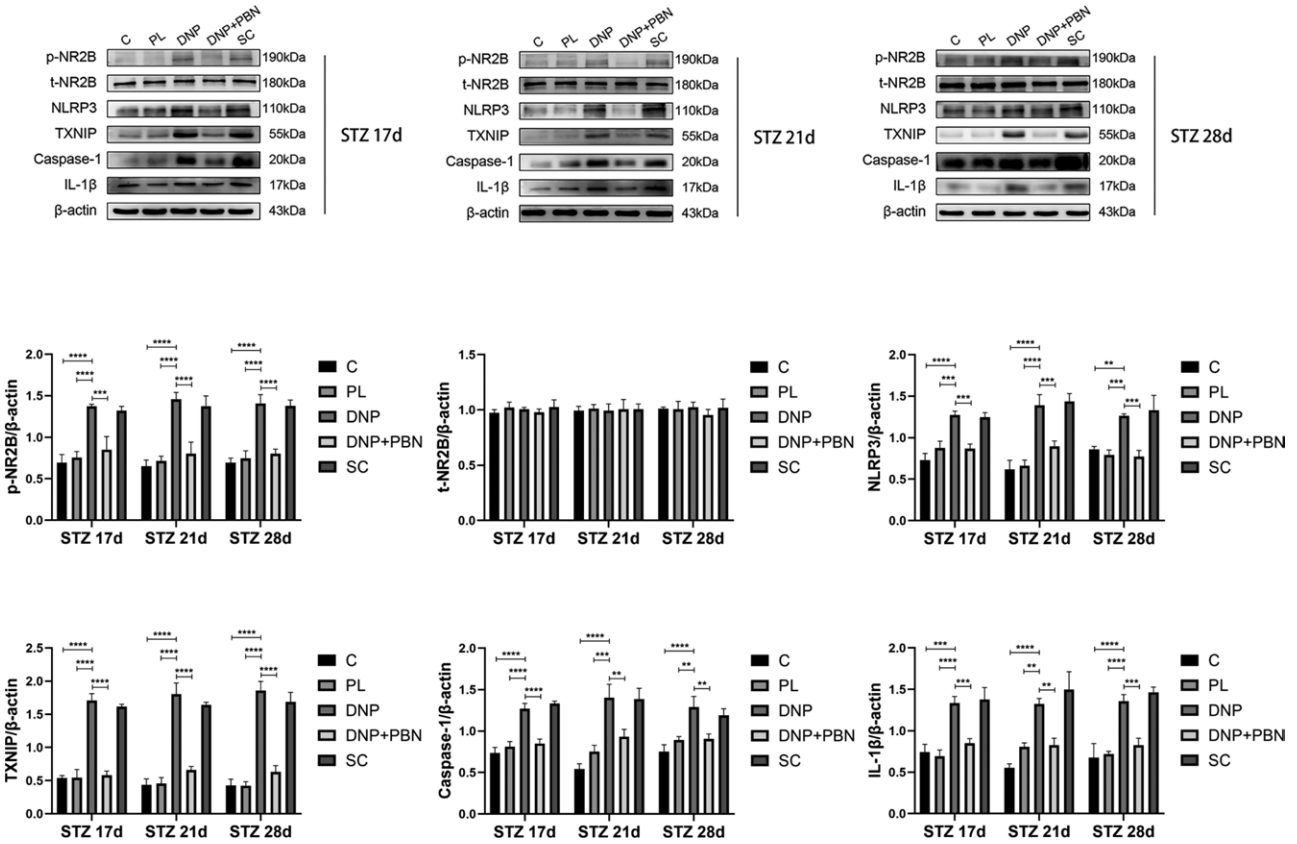

Figure 2. PBN decreased phosphorylation of NR2B, activation of the NLRP3 inflammasome, and the protein levels of TXNIP and IL-1β in spinal cords of DNP rats. The protein levels of p-NR2B, t-NR2B, NLRP3, TXNIP, caspase-1, and IL-1β were compared among the rats in each group on days 17, 21, and 28 after STZ intraperitoneal injection. (Mean ± standard deviation. n = 3. $^{**}P < .01$, $^{***}P < .001$, $^{****}P < .0001$. p-NR2B: DNP group versus DNP + PBN group, $^{***}P = .0003$ [STZ 17 d]. DNP group versus SC group: $P = .9543$ [STZ 17 d], .8428 [STZ 21 d], and .9894 [STZ 28 d]; t-NR2B: DNP group versus C group, $P = .8467$ [STZ 17 d], .9983 [STZ 28 d], and $P > .9999$ [STZ 21 d]. DNP group versus PL group, $P = .9944$ [STZ 17 d], .9955 [STZ 21 d], and .9960 [STZ 28 d]. DNP group versus DNP + PBN group, $P = .9108$ [STZ 17 d], .9981 [STZ 21 d], and .5789 [STZ 28 d]. DNP group versus SC group, $P = .9786$ [STZ 17 d], .9987 [STZ 21 d], and >.9999 [STZ 28 d]; NLRP3: DNP group versus C group, $^{**}P = .0024$ [STZ 28 d]. DNP group versus PL group, $^{***}P = .0002$ [STZ 17 d] and .0007 [STZ 28 d]. DNP group versus DNP + PBN group, $^{***}P = .0001$ [STZ 17 d], .0006 [STZ 21 d], and .0005 [STZ 28 d]. DNP group versus SC group: $P = .9906$ [STZ 17 d], .9697 [STZ 21 d], and .8808 [STZ 28 d]; TXNIP: DNP group versus SC group, $P = .6409$ [STZ 17 d], .3346 [STZ 21 d], and .3812 [STZ 28 d]; caspase-1: DNP group versus PL group, $^{***}P = .0002$ [STZ 21 d] and $^{**}P = .0011$ [STZ 28 d]. DNP group versus DNP + PBN group, $^{**}P = .0026$ [STZ 21 d] and .0015 [STZ 28 d]. DNP group versus SC group: $P = .6750$ [STZ 17 d], .9997 [STZ 21 d], and .5942 [STZ 28 d]; IL-1β: DNP group versus C group, $^{***}P = .0001$ [STZ 17 d]. DNP group versus PL group, $^{**}P = .0015$ [STZ 21 d]. DNP group versus DNP + PBN group, $^{***}P = .0007$ [STZ 17 d] and .0004 [STZ 28 d], $^{**}P = .0019$ [STZ 21 d]. DNP group versus SC group: $P = .9775$ [STZ 17 d], .3756 [STZ 21 d], and .6578 [STZ 28 d]. Tukey post hoc test after 1-way ANOVA.) ANOVA indicates analysis of variance; C group, control group; caspase-1, cysteinyl aspartate-specific proteinase-1; DNP group, diabetic neuropathic pain group; IL-1β, interleukin-1β; NLRP3, NOD-like receptor protein 3; PL group, painless group; p-NR2B, NR2B phosphorylation at Tyr1472; SC group, solvent control group; STZ, streptozotocin; t-NR2B, total NR2B; TXNIP, thioredoxin-interacting protein.

The Localization of NLRP3 and Coupling of TXNIP to NLRP3 in the Spinal Cord

The dual-labeled immunofluorescence of NLRP3 with a microglia marker Iba, a neuron marker NeuN, or an astrocyte marker GFAP showed that NLRP3 was located in microglia and neurons, not in astrocytes of the spinal cord (Figure 3A). We further determined whether ROS activated NLRP3 inflammasome via the coupling of NLRP3 to TXNIP. TXNIP was coexpressed with NLRP3 in the spinal cord (Figure 3B), and the abundance of NLRP3-bound TXNIP was remarkably enhanced in spinal cords of DNP rats compared with rats in control group and painless group. Systematic administration of PBN blocked this enhancement (Figure 3C).

Knockdown of Spinal TXNIP Mitigated Nociceptive Hypersensitivity and Decreased Protein Expression of Spinal p-NR2B via Inhibition of NLRP3 Inflammasome Activation in DNP Rats

Finally, to investigate whether TXNIP was implicated in the DNP process, we knocked down TXNIP through intrathecal injection of specific siRNA for TXNIP. Negative control siRNA was used as control. As expected, TXNIP siRNA significantly reduced the protein level of spinal TXNIP, whereas negative control siRNA did not affect protein expression of TXNIP. In addition, intrathecal injection of TXNIP siRNA reduced spinal protein expression of NLRP3, caspase-1, IL-1β, and p-NR2B in DNP rats (Figure 4). Negative control

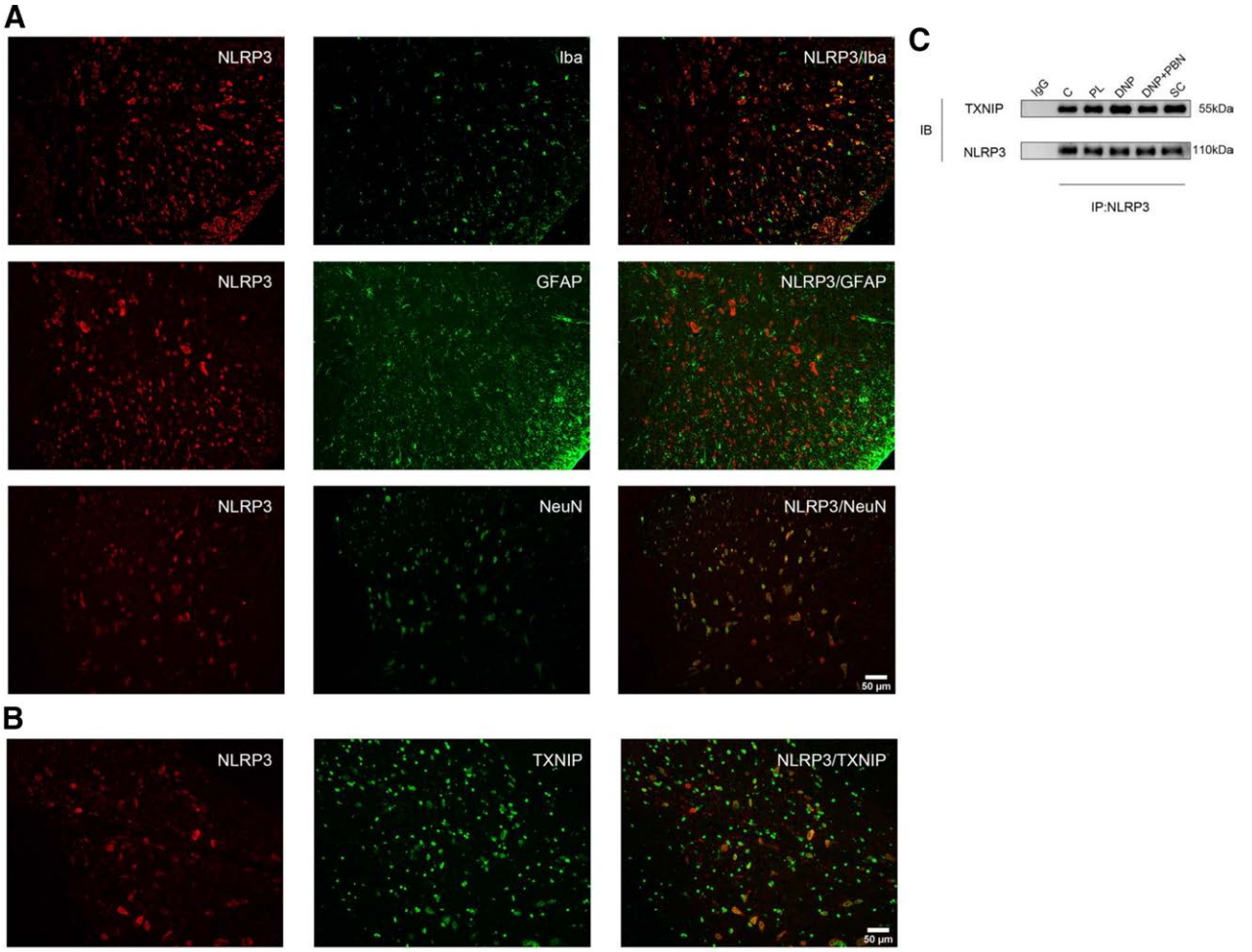

Figure 3. The location of NLRP3 and the interaction of TXNIP to NLRP3 in spinal cord dorsal horn. A, Immunofluorescence showed that NLRP3 colocated with microglia and neurons, not in astrocytes of spinal cord. B, Immunofluorescence showed that NLRP3 colocated with TXNIP in spinal cord dorsal horn. C, Changes of the coupling of TXNIP to NLRP3 in spinal cords of rats in each group. C group indicates control group; DNP group, diabetic neuropathic pain group; GFAP, glial fibrillary acidic protein; Iba, ionized calcium-binding adaptor protein; NeuN, neuronal nuclei; NLRP3, NOD-like receptor protein 3; PL group, painless group; SC group, solvent control group; TXNIP, thioredoxin-interacting protein.

siRNA did not affect the levels of these molecules and nociceptive hypersensitivity in DNP rats.

High-Glucose Treatment Increased the Protein Levels of NLRP3, TXNIP, Caspase-1, and IL-1β in BV2 Cells but Did Not Affect the Protein Expression of p-NR2B in PC12 Cells

The activation of microglia is powered by glycolysis, which relies on high levels of glucose uptake.[24] The activated microglia contribute to central sensitization by producing proinflammatory cytokines to modulate the function of NMDAR in neuron.[25] To determine the mechanisms by which microglia were activated by a high-glucose environment and the interaction between microglia and neurons, we carried out BV2 cell culture and PC12 cell culture. The protein levels of NLRP3, TXNIP, caspase-1, and IL-1β in BV2 cells increased in a high-glucose treatment (Figure 5A). However, high-glucose treatment did not change the protein expression of p-NR2B and t-NR2B in PC12 cells (Figure 5B). There were no significant differences in the levels of these proteins in BV2 cells and PC12 cells between normal control group and osmotic pressure control group (Figure 5), suggesting that the influence of osmotic pressure could be excluded. These results demonstrate that high-glucose treatment can activate BV2 cells, not PC12 cells.

PBN Blocked the Increase of ROS, NLRP3, TXNIP, and IL-1β in BV2 Cells and p-NR2B in PC12 Cells After Coculture of BV2 Cells and PC12 Cells in a High-Glucose Treatment

To further explore the interaction between microglia and neurons, a coculture model was established. Surprisingly, we found that the activated BV2 cells were critical to upregulate the protein expression of p-NR2B in PC12 cells. The level of ROS, protein levels of NLRP3, TXNIP, caspase-1, and IL-1β in BV2 cells in high-glucose group significantly increased compared with normal control group. However, PBN reversed

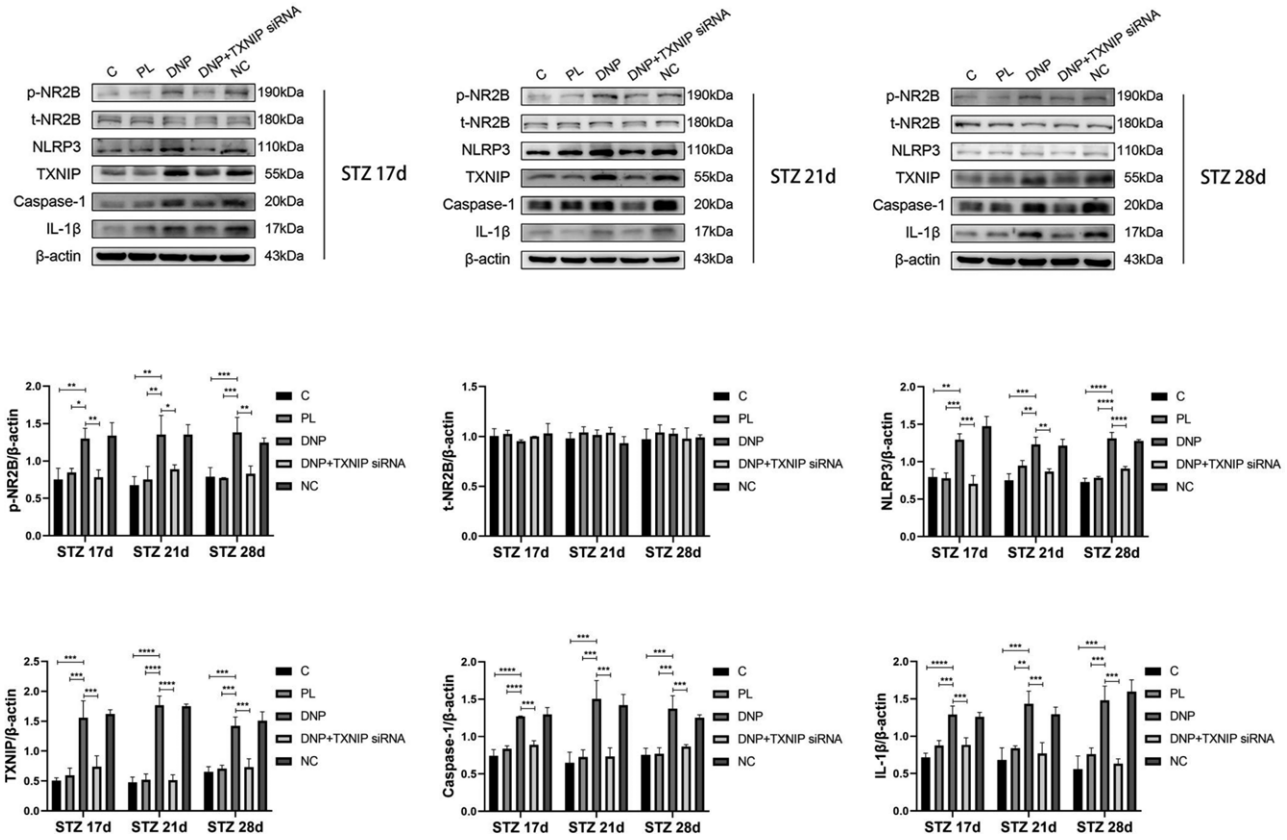

Figure 4. Knockdown of spinal cord TXNIP decreased p-NR2B via NLRP3 inflammasome in spinal cords of DNP rats. The protein levels of p-NR2B, t-NR2B, NLRP3, TXNIP, caspase-1, and IL-1β were compared among the rats in each group on days 17, 21, and 28 after STZ intraperitoneal injection. (Mean ± standard deviation. n = 3. *P < .05, **P < .01, ***P < .001, ****P < .0001; p-NR2B: DNP group versus C group, **P = .0028 [STZ 17 d] and .0032 [STZ 21 d], ***P = .0008 [STZ 28 d]. DNP group versus PL group, *P = .0103 [STZ 17 d], **P = .0074 [STZ 21 d], ***P = .0006 [STZ 28 d]. DNP group versus DNP + TXNIP siRNA group, **P = .0042 [STZ 17 d] and .0013 [STZ 28 d], *P = .0353 [STZ 21 d]. DNP group versus NC group, P = .9954 [STZ 17 d], .6410 [STZ 28 d], and P > .9999 [STZ 21 d]; t-NR2B: DNP group versus C group, P = .7793 [STZ 17 d], .9439 [STZ 21 d], and .9078 [STZ 28 d]. DNP group versus PL group, P = .5261 [STZ 17 d], .9816 [STZ 21 d], and .9994 [STZ 28 d]. DNP group versus DNP + TXNIP siRNA group, P = .8333 [STZ 17 d], .9854 [STZ 21 d], and .9317 [STZ 28 d]. DNP group versus NC group, P = .4728 [STZ 17 d], .4371 [STZ 21 d], and .9749 [STZ 28 d]; NLRP3: DNP group versus C group, **P = .0010 [STZ 17 d], ***P = .0002 [STZ 21 d]. DNP group versus PL group, ***P = .0008 [STZ 17 d], **P = .0086 [STZ 21 d]. DNP group versus DNP + TXNIP siRNA group, ***P = .0003 [STZ 17 d], **P = .0014 [STZ 21 d]. DNP group versus NC group, P = .2853 [STZ 17 d], .9986 [STZ 21 d], and .9021 [STZ 28 d]; TXNIP: DNP group versus C group, ***P = .0001 [STZ 17 d] and .0001 [STZ 28 d]. DNP group versus PL group, ***P = .0002 [STZ 17 d] and .0002 [STZ 28 d]. DNP group versus DNP + TXNIP siRNA group, ***P = .0008 [STZ 17 d] and .0003 [STZ 28 d]. DNP group versus NC group, P = .9894 [STZ 17 d], .9994 [STZ 21 d], and .9038 [STZ 28 d]; caspase-1: DNP group versus C group, ***P = .0004 [STZ 21 d] and .0001 [STZ 28 d]. DNP group versus PL group, ***P = .0009 [STZ 21 d] and .0001 [STZ 28 d]. DNP group versus DNP + TXNIP siRNA group, ***P = .0002 [STZ 17 d], .0010 [STZ 21 d], and .0006 [STZ 28 d]. DNP group versus NC group, P = .9840 [STZ 17 d], .9607 [STZ 21 d], and .5746 [STZ 28 d]; IL-1β: DNP group versus C group, ***P = .0003 [STZ 21 d] and .0001 [STZ 28 d]. DNP group versus PL group, ***P = .0007 [STZ 17 d] and .0008 [STZ 28 d], **P = .0017 [STZ 21 d]. DNP group versus DNP + TXNIP siRNA group, ***P = .0009 [STZ 17 d], .0007 [STZ 21 d], and .0002 [STZ 28 d]. DNP group versus NC group, P = .9926 [STZ 17 d], .6838 [STZ 21 d], and .8543 [STZ 28 d]. Tukey post hoc test after 1-way ANOVA.) ANOVA indicates analysis of variance; C group, control group; caspase-1, cysteinyl aspartate-specific proteinase-1; DNP group, diabetic neuropathic pain group; IL-1β, interleukin-1β; NC group, negative control of siRNA group; NLRP3, NOD-like receptor protein 3; PL group, painless group; p-NR2B, NR2B phosphorylation at Tyr1472; STZ, streptozotocin; t-NR2B, total NR2B; TXNIP, thioredoxin-interacting protein.

the production of these molecules (Figure 6A, B). The level of IL-1β in the cell supernatant was examined at the same time. IL-1β secretion significantly increased in BV2 cells in high-glucose group compared with normal control group. PBN decreased the IL-1β secretion in BV2 cells in PBN group. The DMSO did not affect the IL-1β secretion of BV2 cells in solvent control group (Figure 6C). The protein level of NLRP3-bound TXNIP in BV2 cells increased in high-glucose group compared to normal control group. In PBN group, the combination of TXNIP and NLRP3 in BV2 cells was blocked (Figure 6D). Furthermore, the protein expression of p-NR2B in PC12 cells in high-glucose cocultured group significantly increased compared with normal control cocultured group. PBN treatment could reverse the increased protein expression of p-NR2B in PC12 cells in PBN cocultured group after cocultivation of BV2 cells and PC12 cells (Figure 6E). However, the protein expression of t-NR2B of PC12 cells in all treated groups was not different. The levels of these molecules in BV2 cells and PC12 cells between high-glucose cocultured group and solvent control cocultured group did not differ (Figure 6).

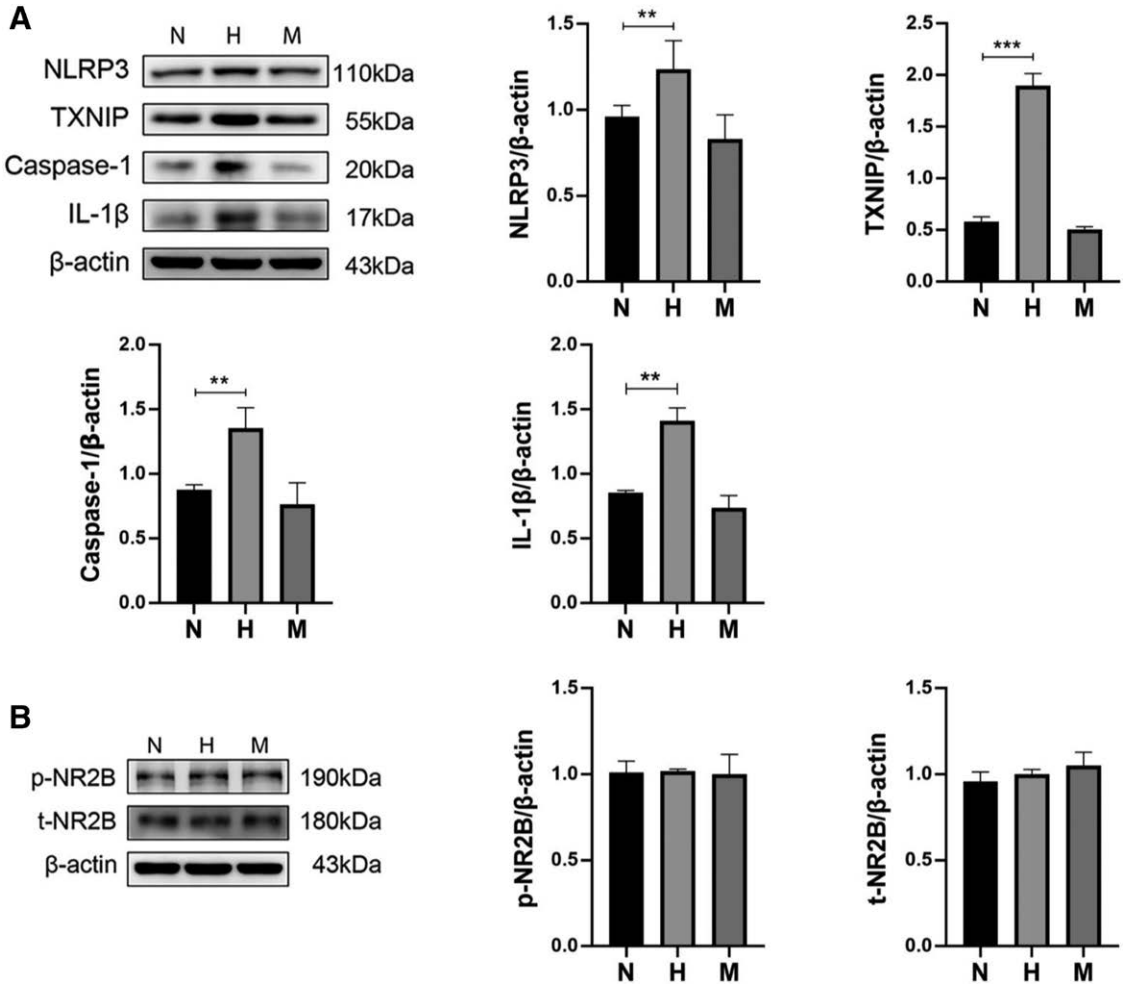

Figure 5. High-glucose treatment increased the protein levels of NLRP3, TXNIP, caspase-1, and IL-1β in BV2 cells but did not affect the protein expression of p-NR2B in PC12 cells. A, The protein levels of NLRP3 (n = 6), TXNIP (n = 4), caspase-1 (n = 5), and IL-1β (n = 4) in BV2 cells in each group. (Mean ± standard deviation. Normal control group versus high-glucose group: NLRP3 [**P = .0073], TXNIP [***P = .0009], caspase-1 [**P = .0040], IL-1β [**P = .0052]; normal control group versus osmotic pressure control group: NLRP3 [P = .2166], TXNIP [P = .1021], caspase-1 [P = .4712], and IL-1β [P = .1217]. Tukey post hoc test after 1-way repeated measures ANOVA.) B, The protein expression of p-NR2B and t-NR2B of PC12 cells in each group. (Mean ± standard deviation. n = 4. Normal control group versus high-glucose group: p-NR2B [P = .9640], t-NR2B [P = .3920]; normal control group versus osmotic pressure control group: p-NR2B [P = .9943], t-NR2B [P = .4266]. Tukey post hoc test after 1-way repeated measures ANOVA.) ANOVA indicates analysis of variance; caspase-1, cysteinyl aspartate-specific proteinase-1; H group, high-glucose group; IL-1β, interleukin-1β; M group, osmotic pressure control group; N group, normal control group; NLRP3, NOD-like receptor protein 3; p-NR2B, NR2B phosphorylation at Tyr1472; t-NR2B, total NR2B; TXNIP, thioredoxin-interacting protein.

DISCUSSION

The findings in the present study include that (1) ROS promoted the activation of the TXNIP-NLRP3 pathway in the spinal cord during the development of DNP; (2) TXNIP promoted NLRP3 inflammasome activation, IL-1β secretion, and phosphorylation of NR2B in spinal cords of DNP rats; and (3) spinal inhibition of ROS or knockdown of TXNIP alleviated nociceptive hypersensitivity in DNP rats.

Given that type 2 diabetes represent over 90% of diabetes, the present study was to investigate the function of the ROS-TXNIP-NLRP3-NR2B pathway in HFSD/STZ-induced type 2 diabetic rat model.

The level of cellular ROS is stable in a dynamic equilibrium. This balance is disrupted under pathological conditions such as inflammatory diseases, neurologic diseases, and diabetes.[26] Cumulative evidence has revealed that oxidative dysfunction is critically involved in the induction and maintenance of neuropathic pain.[27,28] The present study demonstrated that ROS was critical to the development of DNP and ROS scavenger PBN alleviated the mechanical allodynia and thermal hyperalgesia in DNP rats. Recent studies have shown that loss of intraepidermal nerve fibers (IENFs) of the skin is observed in diabetic neuropathy. Mitochondrial dysfunction is associated with several neurodegenerative diseases such as diabetic neuropathy.[29] The relationship between ROS and IENFs in type 2 DNP needs further study.

TXNIP, a redox-dependent inhibition of TRX, plays a key role in metabolic syndromes. TXNIP dissociates with TRX and binds to NLRP3 in the presence

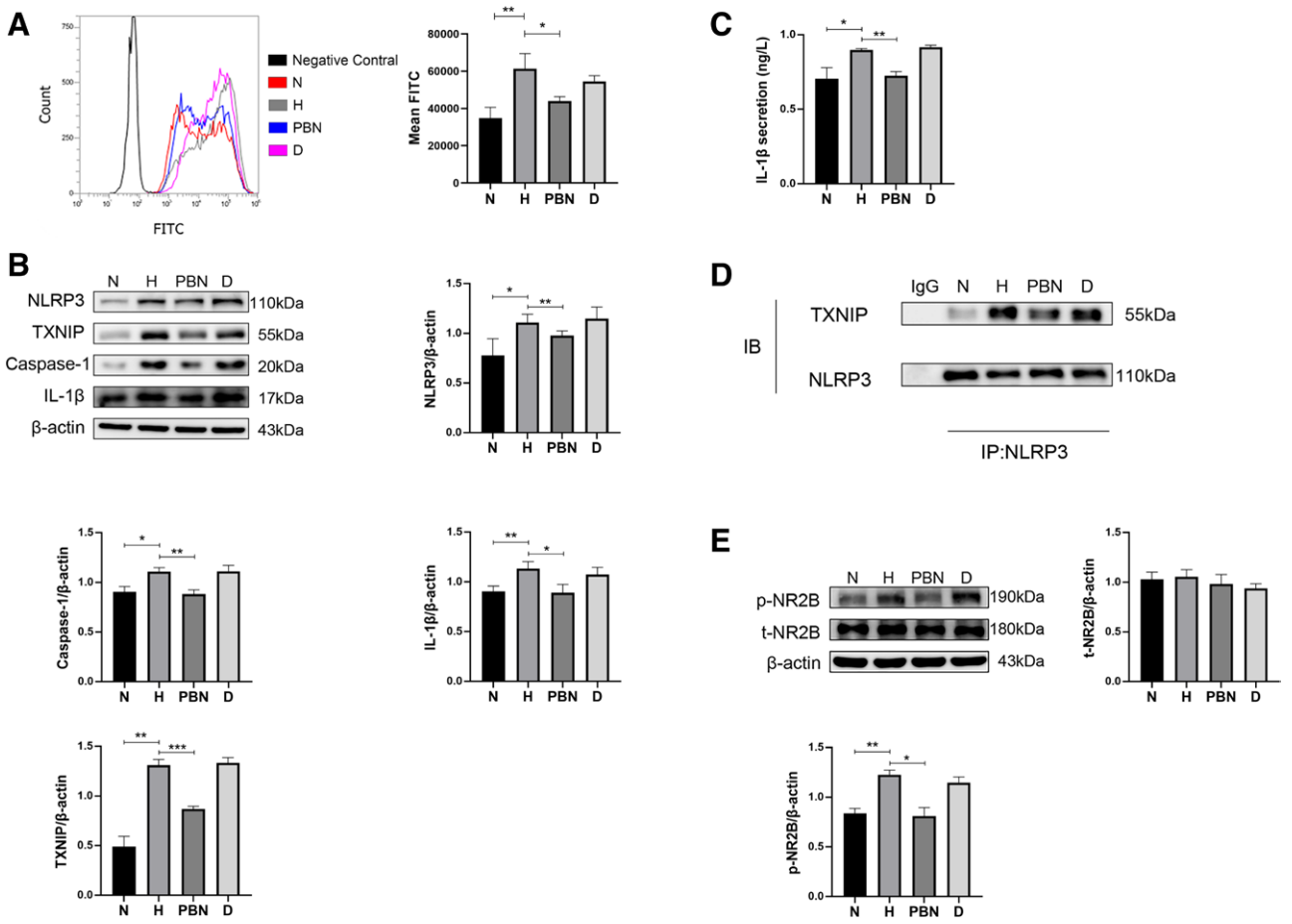

Figure 6. The level of ROS and protein levels of NLRP3, TXNIP, caspase-1, IL-1β; the secretion of IL-1β and the interaction between TXNIP and NLRP3 in BV2 cells; and the protein expression of p-NR2B in PC12 cells increased after coculture of BV2 cells and PC12 cells, and PBN blocked these increases. A, The flow cytometry assay revealed the level of ROS of BV2 cells in each group. (Mean ± standard deviation. n= 6. Normal control group versus high-glucose group: $^{**}P = .0079$; high-glucose group versus PBN group: $^{*}P = .0341$; high-glucose group versus solvent control group: $P = .4532$; Tukey post hoc test after 1-way repeated measures ANOVA.) B, The protein levels of NLRP3 (n = 7), TXNIP (n = 4), caspase-1 (n = 5), and IL-1β (n = 6) of BV2 cells in each group. (Mean ± standard deviation. Normal control group versus high-glucose group: NLRP3 [$^{*}P = .0334$], TXNIP [$^{**}P = .0054$], caspase-1 [$^{*}P = .02$], and IL-1β [$^{**}P = .0032$]; high-glucose group versus PBN group: NLRP3 [$^{**}P = .0043$], TXNIP [$^{***}P = .0008$], caspase-1 [$^{**}P = .0095$], and IL-1β [$^{*}P = .0302$]; high-glucose group versus solvent control group: NLRP3 [$P = .8732$], TXNIP [$P = .9343$], caspase-1 [$P = .9999$], and IL-1β [$P = .6307$]. Tukey post hoc test after 1-way repeated measures ANOVA.) C, The secretion of IL-1β of BV2 cells in each group. (Mean ± standard deviation. n = 4. Normal control group versus high-glucose group: $^{*}P = .0273$; high-glucose group versus PBN group: $^{**}P = .0014$; high-glucose group versus solvent control group: $P = .1370$. Tukey post hoc test after 1-way repeated measures ANOVA.) D, Changes in the coupling of TXNIP to NLRP3 of BV2 cells in each group. E, The protein expression of p-NR2B and t-NR2B of PC12 cells in each group after coculture of BV2 cells and PC12 cells. (Mean ± standard deviation. n = 4. Normal control cocultured group versus high-glucose cocultured group: p-NR2B [$^{**}P = .0017$], t-NR2B [$P = .8341$]; high-glucose cocultured group versus PBN cocultured group: p-NR2B [$^{*}P = .0226$], t-NR2B [$P = .8196$]; high-glucose cocultured group versus solvent control cocultured group: p-NR2B [$P = .2849$], t-NR2B [$P = .2776$]. Tukey post hoc test after 1-way repeated measures ANOVA.) ANOVA indicates analysis of variance; caspase-1, cysteinyl aspartate-specific proteinase-1; D group, solvent control group (BV2 cells), solvent control cocultured group (PC12 cells); H group, high-glucose group (BV2 cells), high-glucose cocultured group (PC12 cells); IL-1β, interleukin-1β; mean FITC, mean fluorescence of fluorescein isothiocyanate; N group, normal control group (BV2 cells), normal control cocultured group (PC12 cells); NLRP3, NOD-like receptor protein 3; PBN group, PBN group (BV2 cells), PBN cocultured group (PC12 cells); p-NR2B, NR2B phosphorylation at Tyr1472; t-NR2B, total NR2B; TXNIP, thioredoxin-interacting protein.

of high concentrations of ROS.[19] The N-acetylcysteine, a ROS scavenger, suppressed the protein expression of NLRP3, TXNIP, and caspase-1.[22] The mitoQ, an antioxidant targeting mitochondrial reactive oxygen species (mtROS), inhibited NLRP3 inflammasome activation and IL-1β maturation by blocking the interaction between TXNIP and NLRP3.[30] Consistent with these studies, the present study demonstrated that ROS increased protein levels of TXNIP, NLRP3, caspase-1, IL-1β, and p-NR2B, and ROS scavenger PBN inhibited this increase in type 2 DNP rats. Given that NLRP3 was not located in astrocytes of the spinal cord of type 2 DNP rats, the cell culture experiments were to determine the interaction between microglia and neurons. BV2 cells and PC12 cells were cultured in a medium with D-glucose (5.5 or 35 mM), which are similar to in vivo levels of blood glucose under "normal" condition or "hyperglycemia hyperosmolar

status" condition. The protein expression of p-NR2B did not increase in PC12 cells cultured in a high-glucose environment. However, the protein expression of spinal p-NR2B increased in type 2 DNP rats. We hypothesized that the activation of microglia in hyperglycemia might be involved. To further investigate the interaction between microglia and neurons, we developed a coculture of BV2 cells and PC12 cells model. The cell culture experiments in the present study demonstrated that the activation of ROS-TXNIP-NLRP3 pathway and IL-1β secretion in cocultured BV2 cells promoted the protein expression of p-NR2B in cocultured PC12 cells in a high-glucose environment and PBN blocked this increase. However, the cell culture medium cannot fully simulate the environment in vivo. In the present study, both in vivo and in vitro experiments were performed to verify the role of the ROS-TXNIP-NLRP3-NR2B pathway in type 2 DNP.

Danger signals such as the cytosolic innate immune signaling receptor NLRP3 are a hallmark of many inflammatory diseases. Once activated, NLRP3 nucleates the assembly of an inflammasome, leading to caspase-1 mediated IL-1β activation and inducing inflammatory and pyroptotic cell death. ROS is essential for NLRP3 inflammasome activation.[31] Abundant evidence indicates that TXNIP is essential for NLRP3 inflammasome activation. NF-κB p65 induced inflammatory response by activation of TXNIP-NLRP3 inflammasome pathway, aggravating the neuropathic pain in chronic constriction injury (CCI) rats and primary microglial cells.[32] Moreover, the loganin, an iridoid glycoside, prevented TXNIP activation, resulting in decreased NLPR3 inflammasome and IL-1β in CCI rats.[33] However, NLRP3 is a critical mediator of IL-1β release in macrophages while TXNIP is not.[34] The function of the ROS-TXNIP-NLRP3 pathway in type 2 DNP is still unknown. To determine the role of TXNIP-induced NLRP3 inflammasome activation in type 2 DNP, we further demonstrated that TXNIP was essential for NLRP3 inflammasome activation and contributed to the development of type 2 DNP. TXNIP siRNA inhibited the protein expression of NLRP3, caspase-1, IL-1β, and p-NR2B in the spinal cord and alleviated the mechanical allodynia and thermal hyperalgesia in type 2 DNP rats. Furthermore, a few studies have reported the role of TXNIP in CCI-induced and partial sciatic nerve ligation-induced neuropathic pain.[21,32] Whether TXNIP plays a role in other neuropathic pain needs more research.

Spinal cord central sensitization plays a vital role in chronic neuropathic pain. The activation of the spinal NMDA receptor produces hypersensitivity of spinal neurons, subsequently resulting in central sensitization.[35] After peripheral nerve injury, the protein expression of the p-NR2B was significantly upregulated in the spinal cord, although the protein expression of spinal total-NR2B was not altered.[36] Our previous study identified that p-NR2B played a vital role in the development of type 2 DNP.[8]

As a potential underlying mechanism of central sensitization, glial overactivation results in a neuroinflammatory state, characterized by high levels of IL-1β, which increases the excitability of central nervous system neurons.[37] IL-1β regulates the p-NR2B in neurons of the spinal cord via activation of IL-1R.[38] IL-1β activates IL-1RI and recruits myeloid differentiation primary response protein 88 and IL-1R accessory protein to form IL-1R complexes, which are associated with NR2B.[39] The present study revealed that PBN or TXNIP siRNA blocked the increase of protein expression of p-NR2B and IL-1β in the spinal cord and alleviated the mechanical allodynia and thermal hyperalgesia in type 2 DNP rats. The function of IL-1β and IL-1R complexes in type 2 DNP needs further study.

In conclusion, the present study revealed that spinal ROS contributed to type 2 DNP by regulating the TXNIP-NLRP3-NR2B pathway. Phosphorylation of NR2B in the spinal cord led to central sensitization and eventually contributed to type 2 DNP. These results may provide a new therapeutic drug for the treatment of type 2 DNP.

DISCLOSURES

Name: Jun-Wu Wang, BD.
Contribution: This author helped design the study, perform the experiments, collect the data, analyze the data, and write the manuscript.
Name: Xiu-Ying Ye, BD.
Contribution: This author helped design the study, perform the experiments, collect the data, analyze the data, and write the manuscript.
Name: Ning Wei, BD.
Contribution: This author helped perform the experiments and collect the data.
Name: Shi-Shu Wu, BD.
Contribution: This author helped perform the experiments and collect the data.
Name: Zhe-Hao Zhang, BD.
Contribution: This author helped perform the experiments and collect the data.
Name: Guang-Hui Luo, BD.
Contribution: This author helped perform the experiments and collect the data.
Name: Xu Li, PhD.
Contribution: This author helped analyze the data.
Name: Jun Li, PhD, MD.
Contribution: This author helped design the study, analyze the data, and write the manuscript.
Name: Hong Cao, MD.
Contribution: This author helped design the study, analyze the data, and write the manuscript.
This manuscript was handled by: Jianren Mao, MD, PhD.

REFERENCES

1. Aschner P, Karuranga S, James S, et al. The International Diabetes Federation's guide for diabetes epidemiological studies. *Diabetes Res Clin Pract*. 2021;172:108630.

2. Ojo O. Dietary intake and type 2 diabetes. *Nutrients*. 2019;11:2177.
3. Calcutt NA. Diabetic neuropathy and neuropathic pain: a (con)fusion of pathogenic mechanisms? *Pain*. 2020;161(suppl 1):S65–S86.
4. Cohen SP, Mao J. Neuropathic pain: mechanisms and their clinical implications. *BMJ*. 2014;348:f7656.
5. Wang D, Couture R, Hong Y. Activated microglia in the spinal cord underlies diabetic neuropathic pain. *Eur J Pharmacol*. 2014;728:59–66.
6. Matsumura S, Kunori S, Mabuchi T, et al. Impairment of CaMKII activation and attenuation of neuropathic pain in mice lacking NR2B phosphorylated at Tyr1472. *Eur J Neurosci*. 2010;32:798–810.
7. Wu LJ, Zhuo M. Targeting the NMDA receptor subunit NR2B for the treatment of neuropathic pain. *Neurotherapeutics*. 2009;6:693–702.
8. Zhu YB, Jia GL, Wang JW, et al. Activation of CaMKII and GluR1 by the PSD-95-GluN2B coupling-dependent phosphorylation of GluN2B in the spinal cord in a rat model of type-2 diabetic neuropathic pain. *J Neuropathol Exp Neurol*. 2020;79:800–808.
9. Niesters M, Dahan A. Pharmacokinetic and pharmacodynamic considerations for NMDA receptor antagonists in the treatment of chronic neuropathic pain. *Expert Opin Drug Metab Toxicol*. 2012;8:1409–1417.
10. Yamashita A, Matsuoka Y, Matsuda M, Kawai K, Sawa T, Amaya F. Dysregulation of p53 and parkin induce mitochondrial dysfunction and leads to the diabetic neuropathic pain. *Neuroscience*. 2019;416:9–19.
11. Gao X, Kim HK, Mo Chung J, Chung K. Reactive oxygen species (ROS) are involved in enhancement of NMDA-receptor phosphorylation in animal models of pain. *Pain*. 2007;131:262–271.
12. Chen JL, Lu JH, Xie CS, et al. Caveolin-1 in spinal cord modulates type-2 diabetic neuropathic pain through the Rac1/NOX2/NR2B signaling pathway. *Am J Transl Res*. 2020;12:1714–1727.
13. Jia M, Wu C, Gao F, et al. Activation of NLRP3 inflammasome in peripheral nerve contributes to paclitaxel-induced neuropathic pain. *Mol Pain*. 2017;13:1–11.
14. Liu P, Cheng J, Ma S, Zhou J. Paeoniflorin attenuates chronic constriction injury-induced neuropathic pain by suppressing spinal NLRP3 inflammasome activation. *Inflammopharmacology*. 2020;28:1495–1508.
15. Xu L, Wang Q, Jiang W, Yu S, Zhang S. MiR-34c ameliorates neuropathic pain by targeting NLRP3 in a mouse model of chronic constriction injury. *Neuroscience*. 2019;399:125–134.
16. Chen SP, Zhou YQ, Wang XM, et al. Pharmacological inhibition of the NLRP3 inflammasome as a potential target for cancer-induced bone pain. *Pharmacol Res*. 2019;147:104339.
17. An Y, Zhang H, Wang C, et al. Activation of ROS/MAPKs/NF-κB/NLRP3 and inhibition of efferocytosis in osteoclast-mediated diabetic osteoporosis. *FASEB J*. 2019;33:12515–12527.
18. Minutoli L, Puzzolo D, Rinaldi M, et al. ROS-mediated NLRP3 inflammasome activation in brain, heart, kidney, and testis ischemia/reperfusion injury. *Oxid Med Cell Longev*. 2016;2016:2183026.
19. Hwang J, Suh HW, Jeon YH, et al. The structural basis for the negative regulation of thioredoxin by thioredoxin-interacting protein. *Nat Commun*. 2014;5:2958.
20. Jia Y, Cui R, Wang C, et al. Metformin protects against intestinal ischemia-reperfusion injury and cell pyroptosis via TXNIP-NLRP3-GSDMD pathway. *Redox Biol*. 2020;32:101534.
21. Pan Z, Shan Q, Gu P, et al. miRNA-23a/CXCR4 regulates neuropathic pain via directly targeting TXNIP/NLRP3 inflammasome axis. *J Neuroinflammation*. 2018;15:29.
22. Mai W, Xu Y, Xu J, et al. Berberine inhibits Nod-like receptor family pyrin domain containing 3 inflammasome activation and pyroptosis in nonalcoholic steatohepatitis via the ROS/TXNIP axis. *Front Pharmacol*. 2020;11:185.
23. Li CD, Zhao JY, Chen JL, et al. Mechanism of the JAK2/STAT3-CAV-1-NR2B signaling pathway in painful diabetic neuropathy. *Endocrine*. 2019;64:55–66.
24. Wang L, Pavlou S, Du X, Bhuckory M, Xu H, Chen M. Glucose transporter 1 critically controls microglial activation through facilitating glycolysis. *Mol Neurodegener*. 2019;14:2.
25. Ji RR, Nackley A, Huh Y, Terrando N, Maixner W. Neuroinflammation and central sensitization in chronic and widespread pain. *Anesthesiology*. 2018;129:343–366.
26. Yang S, Lian G. ROS and diseases: role in metabolism and energy supply. *Mol Cell Biochem*. 2020;467:1–12.
27. Teixeira-Santos L, Albino-Teixeira A, Pinho D. Neuroinflammation, oxidative stress and their interplay in neuropathic pain: focus on specialized pro-resolving mediators and NADPH oxidase inhibitors as potential therapeutic strategies. *Pharmacol Res*. 2020;162:105280.
28. Gwak YS, Kang J, Unabia GC, Hulsebosch CE. Spatial and temporal activation of spinal glial cells: role of gliopathy in central neuropathic pain following spinal cord injury in rats. *Exp Neurol*. 2012;234:362–372.
29. Fan B, Li C, Szalad A, et al. Mesenchymal stromal cell-derived exosomes ameliorate peripheral neuropathy in a mouse model of diabetes. *Diabetologia*. 2020;63:431–443.
30. Han Y, Xu X, Tang C, et al. Reactive oxygen species promote tubular injury in diabetic nephropathy: the role of the mitochondrial ros-txnip-nlrp3 biological axis. *Redox Biol*. 2018;16:32–46.
31. Mangan MSJ, Olhava EJ, Roush WR, Seidel HM, Glick GD, Latz E. Targeting the NLRP3 inflammasome in inflammatory diseases. *Nat Rev Drug Discov*. 2018;17:588–606.
32. Miao J, Zhou X, Ji T, Chen G. NF-κB p65-dependent transcriptional regulation of histone deacetylase 2 contributes to the chronic constriction injury-induced neuropathic pain via the microRNA-183/TXNIP/NLRP3 axis. *J Neuroinflammation*. 2020;17:225.
33. Cheng KI, Chen SL, Hsu JH, et al. Loganin prevents CXCL12/CXCR4-regulated neuropathic pain via the NLRP3 inflammasome axis in nerve-injured rats. *Phytomedicine*. 2021;92:153734.
34. Masters SL, Dunne A, Subramanian SL, et al. Activation of the NLRP3 inflammasome by islet amyloid polypeptide provides a mechanism for enhanced IL-1β in type 2 diabetes. *Nat Immunol*. 2010;11:897–904.
35. Bannister K, Kucharczyk M, Dickenson AH. Hopes for the future of pain control. *Pain Ther*. 2017;6:117–128.
36. Chen SR, Samoriski G, Pan HL. Antinociceptive effects of chronic administration of uncompetitive NMDA receptor antagonists in a rat model of diabetic neuropathic pain. *Neuropharmacology*. 2009;57:121–126.
37. Nijs J, Loggia ML, Polli A, et al. Sleep disturbances and severe stress as glial activators: key targets for treating central sensitization in chronic pain patients? *Expert Opin Ther Targets*. 2017;21:817–826.
38. Gao YJ, Ji RR. Targeting astrocyte signaling for chronic pain. *Neurotherapeutics*. 2010;7:482–493.
39. Gardoni F, Boraso M, Zianni E, et al. Distribution of interleukin-1 receptor complex at the synaptic membrane driven by interleukin-1β and NMDA stimulation. *J Neuroinflammation*. 2011;8:14.